RECENT RESULTS FOR RANDOM NETWORKS OF AUTOMATA*

By H. Flyvbjerg

The Niels Bohr Institute, University of Copenhagen, Blegdamsvej 17, 2100 Copenhagen Ø, Denmark

(Received October 3, 1988)

After a brief historical and contextual introduction to random networks of automata we review recent numerical and analytical results. Open questions and unsolved problems are pointed out and discussed. One such question is also answered; it is shown that the size of *the stable core* can be used as order parameter for a transition between phases of *frozen* and *chaotic* network behavior. A mean-field-like but exact self-consistency equation for the size of the stable core is given. A new derivation of critical parameter values follows from it.

PACS numbers: 05.90.+m

1. Introduction

Random networks of automata have recently received some attention from workers in theory of automata, in neural networks, and in disordered systems. They were introduced by S. Kauffman as simplified models for the complex genetic regulatory system that guides cell differentiation in embryonic development, and ensures metabolic stability; see Sect. 2. Compared with the regular networks of automata studied by Wolfram and others, random networks differ by being non-homogeneous and infinite dimensional; see Sect. 3. Compared with spin glass models for neural networks, random networks are more primitive objects, which in some ways resemble spin glasses more than they resemble neural networks, see Sect. 4. In Sect. 5 the *stable core* of a random network is defined. A mean-field-like but exact self-consistency equation for its size is derived, and from this equation critical parameter values are found. This is a new, promising approach: it appears that critical exponents and many network properties in the frozen phase may be computed as due to fluctuations in the size of the stable core. Also, the self-consistency equation may be generalized to give the distribution of local magnetizations. In Sect. 6 Monte Carlo results for random networks are reviewed and compared with analytical results for spin glasses. Section 7 presents analytical calculations for a special case: the totally connected random network. One characteristic probability distribution is found from its moments, another is found numerically from a stochastic recursion relation. Several other results for this case are reviewed.

* Presented at the XXVIII Cracow School of Theoretical Physics, Zakopane, Poland, May 31 — June 10, 1988.

Section 8 presents another analytically tractable case: that of connectivity one. It is explained why many quantities are analytically computable in this case, and a number of results are reviewed. Section 9 contains the conclusions.

2. *Kauffman's model*

In Fig. 1 each circle represents a chemical reaction. Each reaction depends on other reactions in the same environment. Dependence between reactions is denoted by an arrow going into the dependent reaction. To keep things as simple as possible we shall say that reaction no. i either takes place ($\sigma_i = 1$) or does not take place ($\sigma_i = 0$). We shall also let time be discrete and let the reaction rate σ_i of reaction no. i be a function of the reaction rates $\sigma_{j_1(i)}, \sigma_{j_2(i)}, \ldots, \sigma_{j_K(i)}$ at time t:

$$\sigma_i(t+1) = f_i(\sigma_{j_1(i)}(t), \sigma_{j_2(i)}(t), \ldots, \sigma_{j_K(i)}(t)). \tag{1}$$

Here $j_1(i), \ldots, j_K(i)$ are the numbers of the reactions that reaction no. i depends on. f_i can be any Boolean function, since the products of, e.g., reaction number $j_1(i)$ may either be necessary for reaction no. i, or they may inhibit it. And they may have this effect in a way that depends on the values of $\sigma_{j_2(i)}, \ldots, \sigma_{j_K(i)}$. So while we have kept the description of the individual reaction as simple as possible, we have left their possible interdependencies wide open.

If we were to describe a specific network of N chemical reactions, we would have to specify the dependencies $(j_1(i), \ldots, j_K(i))_{i=1,\ldots,N}$ and the Boolean functions $(f_i)_{i=1,\ldots,N}$. This was not the goal Kauffman set himself, when he formulated his model [1, 2]. He considered

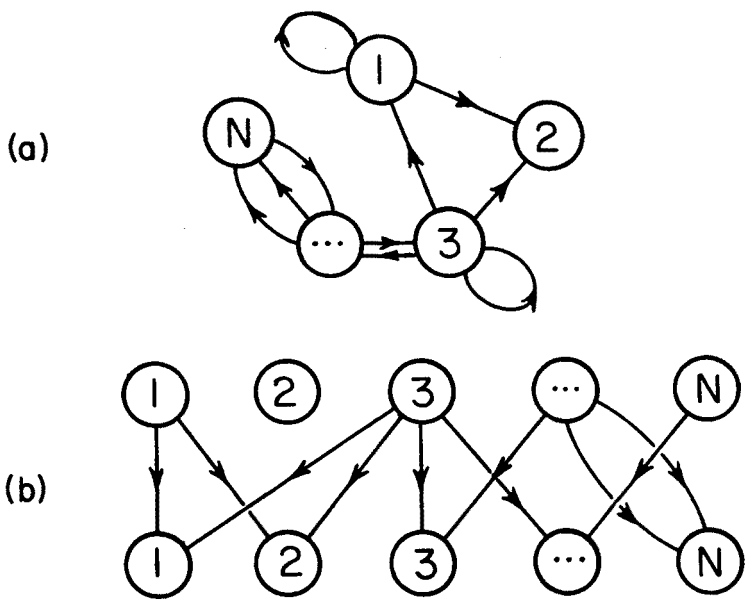

Fig. 1. A random chemical reaction net

the protein synthesis of genes and argued that this process probably is an all-or-none binary process. His goal was to investigate whether metabolic stability and cell differentiation in embryonic development require the genetic system to be precisely constructed: has evolutionary history selected only highly ordered reaction circuits which alone insure metabolic stability, or are stability and differentiation processes to be expected even in nets of randomly interconnected regulatory circuits as the probable consequence of mathematical laws for random networks? Put in other words, the question is: are living things, in the parts that were assembled first in evolution, like *precisely* assembled automata made to a design that is the result of evolutionary selection, or are they like *randomly* assembled automata, whose characteristic behavior reflects their unorderly construction, no matter how evolution selected the surviving forms?

Kauffman addressed this question by studying the statistical properties of randomly assembled Boolean networks: he fixed N and K and chose for each i $j_1(i), \ldots, j_K(i)$ at random in $\{1, 2, \ldots, N\}$. He also chose $f_i(\sigma_1, \ldots, \sigma_K)$ at random in $\{0, 1\}$ for each input $(\sigma_1, \ldots, \sigma_K)$. With a sample network thus defined, he followed the time evolution of random initial configurations on a computer using Eq. (1) for dynamical law. The results he compared with experimental data on living things in the following way: the number N of elements in the random networks is identified with the number of genes per cell in an organism. There is a practical problem in doing this: the estimated number of genes in a cell starts around 2000 with bacteria and ends around 40, 000, 000 with *Trillium*, the small plant which is the "banana fly" of plant genetics. Nets this size one cannot simulate, so the comparison is done mainly with extrapolated simulation data. Quantities compared are: number of cell types per organism with number of different limit cycles per net, see Fig. 2, and cell replication times in organisms with cycle lengths in random nets, see Fig. 3.

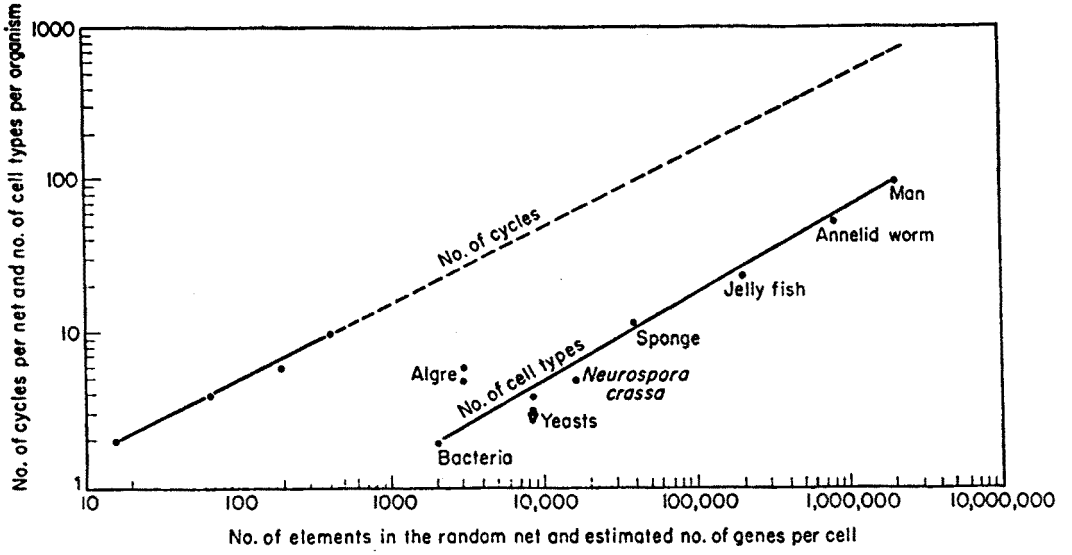

Fig. 2. Log number of cell types plotted against log estimated number of genes. The theoretical curve shows log number state cycles against log N [1]

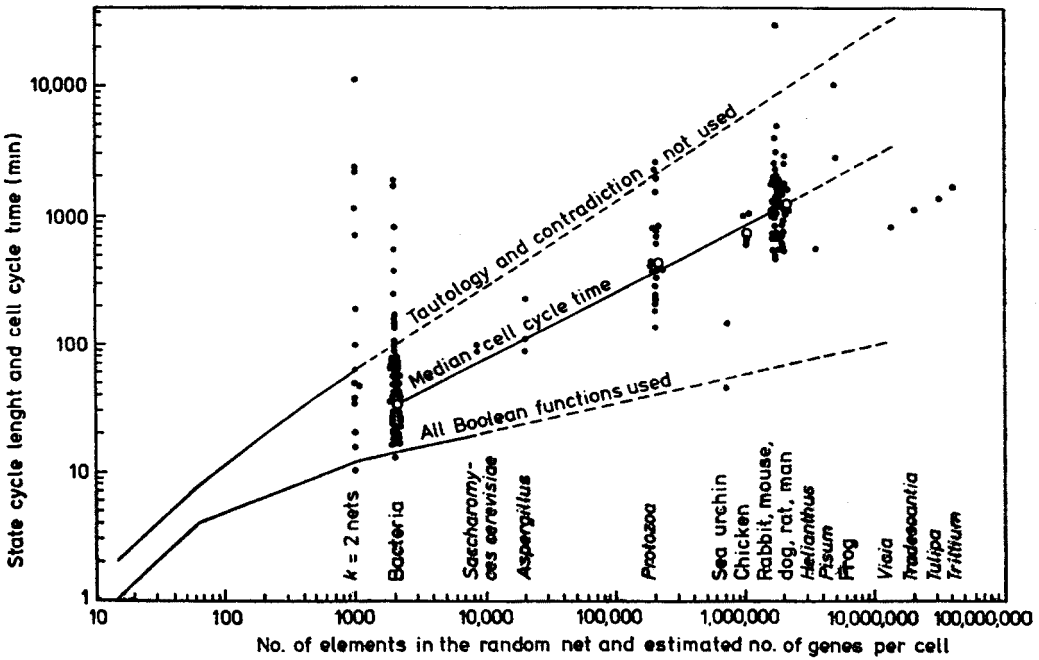

Fig. 3. Correlation between quantity of DNA per cell and cell cycle time. Also plotted is state cycle length as a function of N in $K = 2$ nets either using all 16 Boolean functions of two inputs, or excluding tautology and contradiction [1]

The purpose of this Section was not to convince you that Kauffman's model is the ultimate answer to the mystery of life. It was only meant to explain why a certain class of random Boolean networks is often referred to as "Kauffman's model".

3. Comparison with regular networks of automata

Maybe you are acquainted with the cellular automata studied by Steven Wolfram and others [3]: Boolean variables σ_i are arranged in a regular lattice in 1, 2, or more dimensions and develop in time according to a law like Eq. (1), where $(j_1(i), \ldots, j_K(i))$ fall in a neighbourhood of i which is independent of i, see Fig. 4, and the function f is also chosen not to depend on i[1]. Such regular networks can mimic partial differential equations in a primitive form. Eq. (1) would mimic a first order equation w.r.t. time. Higher order equations are obtained by letting $\sigma_i(t+1)$ depend on variables at time $t, t-1, \ldots$

Fig. 5 shows results obtained with such a regular network of automata [7]: on a 1024 by 512 hexagonal lattice hard spheres move along links or sit on sites, and collide at sites according to simple, deterministic rules that conserve momentum. In each time step a mov-

[1] The intermediate situation, where the variables are arranged in a regular lattice and receive input from their neighbours, but the functions f_i are chosen at random, has been studied [4–6], but will not be discussed here for lack of space.

ing sphere moves one lattice spacing and collides, if there is another sphere to collide with. Boundary conditions are periodic in the vertical direction. Spheres keep coming in through the left boundary with a specified average density and disappear at the right boundary. In the resulting current a flat plate has been inserted. After 5000 time steps the matter flux averaged over 16 by 16 sites is as shown in Fig. 5. One sees a Von Karman street to the right

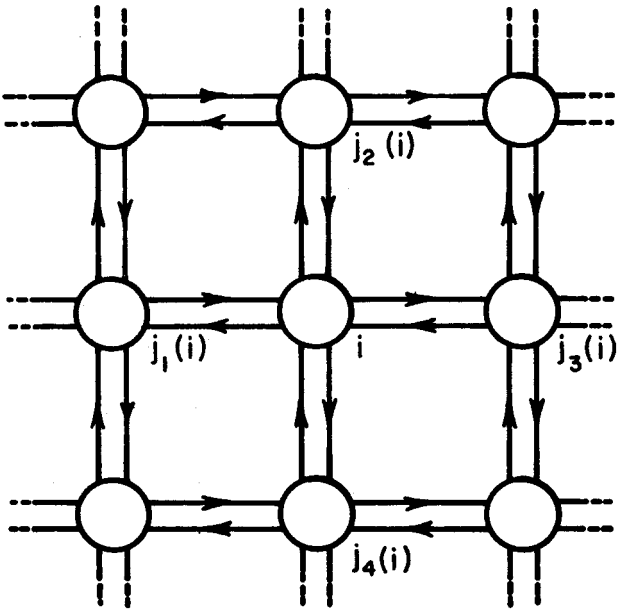

Fig. 4. Automata arranged into square lattice with inputs from nearest neighbours

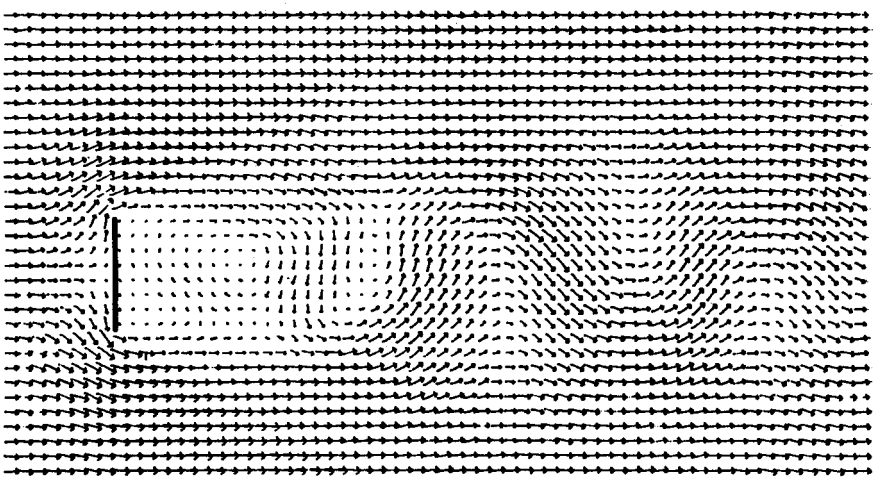

Fig. 5. Two dimensional flow around a plate for a Reynold's number of order 70 after 5,000 time steps. The direction and modulus of arrows are proportional to the mass flux on a 64 by 32 grid [7]

of the plate, as one would, if Navier-Stokes equations were solved with the same boundary conditions.

This primitive network of automata has several advantages over finite element methods applied to Navier-Stokes equations; e.g. high speed of computation, numerical stability, and simple boundary conditions at obstacles inserted in the current [7].

I hope this one example has convinced you that cellular automata can describe physical systems. The reason they are interesting for physics is that they are much easier to program on computers than differential equations are; especially on highly parallel special purpose computers.

Now let us do a simple estimate showing what kind of physical system Kauffman's model is related to: when $(j_1(i), \ldots, j_K(i))$ are chosen as shown in Fig. 4 it is clear that Eq. (1) can propagate a signal across the lattice with a maximal velocity of one lattice spacing per time step. Generalizing to a d-dimensional lattice, the number of variables that can have received a signal from a certain variable grows with time as t^d. On the other hand, when $(j_1(i), \ldots, j_K(i)$ are chosen at random as in Kauffman's model, each variable will on the average send its output to K other variables, each of which sends output to K variables, none of which are identical, when N is infinite, and K is finite. So the number of variables that can have received a signal from a certain variable grows with time as K^t. This exponential growth with time is faster than t^d for any value of d. For this reason randomly connected networks are sometimes called *infinite dimensional* networks. As opposed to finite dimensional networks of automata infinite dimensional networks have received little attention until recently.

An infinite dimensional system may also arise through a mean field description of a finite dimensional system with long range forces. Quenched, random interactions occur in spin glasses. The Sherrington-Kirkpatrick (SK) model is a mean field theory for spin glasses [8]. A number of properties of this model may be computed by the replica method developed by Parisi and collaborators. (For a review see [9].) Since the SK-model and Kauffman's model both are infinite dimensional and have quenched random interactions, let us see what else they have in common. In the thermodynamic limit the configuration space of the SK-model is broken into free energy valleys separated by infinitely high energy barriers. From the Ising model in its magnetized phase you may be familiar with two such valleys: magnetization 'up' and 'down'. The SK-model has an infinity of such valleys, and their relative sizes vary from sample to sample. The quantity $\overline{Y_P}$ expresses this multi-valley structure: the bar means 'sample averaged', and for a given sample Y_P is the probability that P randomly chosen configurations belong to the same valley. Kauffman's model also has a multi-valley structure, and even so for finite N: since configuration space is finite, of size 2^N, any initial configuration will in time develop onto a limit cycle. The set of configurations ending up on the same limit cycle is its *basin of attraction*. So configuration space is broken into basins of attraction of various sizes, see Fig. 6 for a symbolic representation of this picture. This is a multi-valley structure like that of the SK-model, and Y_P is defined for Kauffman's model in obvious analogy with the definition for the SK-model. Fig. 7 shows $\overline{Y_P}$ plotted versus $\overline{Y}_2$ for Kauffman's model with K ranging from 1 to 4 and N ranging from 5 to 240. Each point represents an average over 10,000 samples from a Monte Carlo

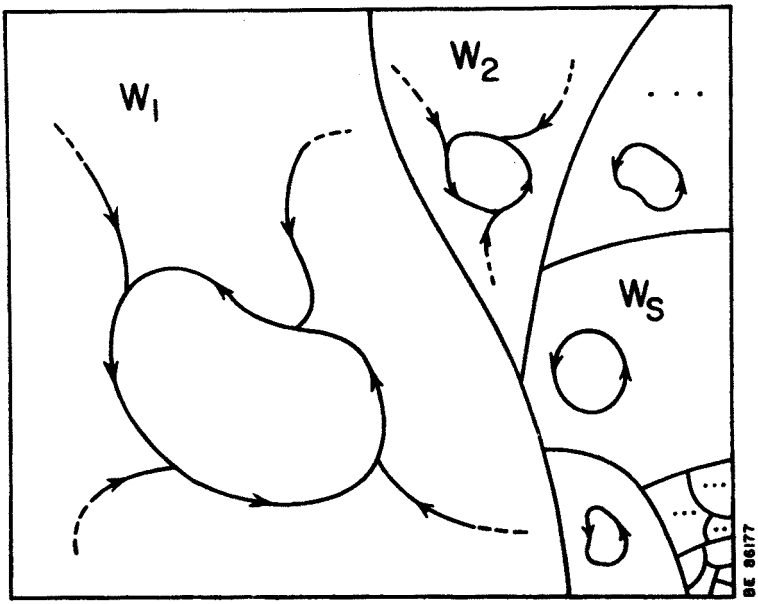

Fig. 6. Highly symbolic representation of configuration space as a rectangle with area 1 broken into basins of attraction with areas W_s, $s = 1, 2, \ldots$, each basin containing a limit cycle as attractor

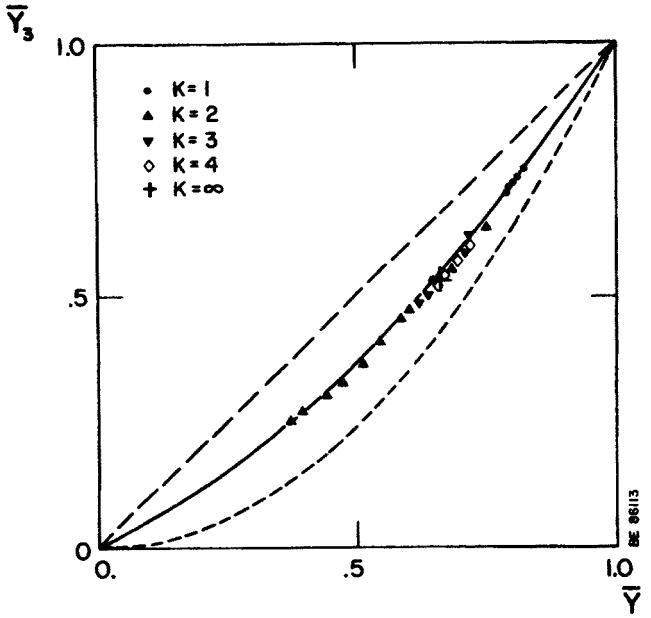

Fig. 7. $\overline{Y}_3$ versus $\overline{Y}$ [10]. Each point represents an average over 10,000 samples. The full curve represents the mean field result for spin glasses: $\overline{Y}_3 = \overline{Y}(1+\overline{Y})/2$. The dashed curves are bounds $\overline{Y}^2 \leqslant \overline{Y}_3 \leqslant \overline{Y}$ that $\overline{Y}_3$ must satisfy

simulation [10]. The line passing through the points is *not* a fit! It is the theoretical relationship for the SK-model [11–14]:

$$\overline{Y}_3 = \overline{Y}_2(1+\overline{Y}_2)/2. \tag{2}$$

An obvious question is: do the points fall on the line? If they do, we have discovered a new law of universality, which connects a thermodynamical system having energy and temperature with a rather primitive deterministic automaton having neither. The answer is given in a subsequent Section.

4. Comparison with neural networks

Take another look at Fig. 1, and let now each circle represent a formal neuron, which may be in one of two states: 'firing', $\sigma_i = 1$, or 'quiescent', $\sigma_i = 0$. When the connectivity K is large, Fig. 1 resembles the pattern of connections in neural network models. So, to clarify similarities and differences, let us compare Kauffman's model with spin glass models for neural networks, like the Hopfield model. (For a recent review see [15].)

Such models attempt at most to describe *local* properties of organic networks, since all neurons are treated equivalently with no directional flow of information through the network. The network may be thought of as a small chunk of 'brain-matter' with its neurons connected in a way that leaves no surface. The functions f_i in Eq. (1) are usually threshold functions depending linearly on the inputs through a connection matrix C, which expresses synaptic efficiencies; e.g.

$$f_i(\sigma) = \theta\Big(\sum_{j=1}^{N} C_{ij}\sigma_j - \theta_i\Big). \tag{3}$$

The synaptic efficiencies C_{ij} and the thresholds θ_i are real variables that adapt in learning processes, whereas the time evolution in Eq. (1) for fixed C_{ij} and θ_i describes a process of recall or association.

The step-function and the linear dependence on σ in Eq. (3) is chosen with an eye on the properties of a real neuron. Very crudely described, it gives a thresholded response to the weighted sum of activity in the neurons it receives input from. This restricts f_i to a limited subset of all Boolean functions of σ, as Eq. (3) shows. This is an essential difference between the networks of Kauffman and Hopfield: Hopfield's network has Boolean variables and, in a dilute version [22], random connections. But even when the learned patterns stored in C_{ij} are random, f_i is not a random Boolean function, as it is in Kauffman's model.

5. The stable core in random Boolean networks [23, 24]

When the number of variables N is infinite, Kauffman's model has two phases: a 'frozen' phase in which almost all variables evolve to a constant value which is independent of the initial configuration, and a 'chaotic' phase in which a finite fraction of variables keep changing their values, and the average length of limit cycles grows exponentially with N. This was first seen in simulations [1, 2]. Then it was proven by looking at the time evolution

of overlaps between configurations in an annealed version of the model [17]. Subsequently the annealed model was shown to be equivalent in the thermodynamic limit to the quenched model described here [18].

In this Section we describe the phase transition using the relative size s of 'the stable core' as order parameter. The stable core is the set of variables σ_i which develop in time to a constant value that is independent of the initial configuration. Any variable σ_i can belong to the stable core for one of $K+1$ mutually exclusive reasons, see Fig. 8:
(0) σ_i is updated with a function f_i which depends on variables $(\sigma_{j_1(i)}, \ldots, \sigma_{jK(i)})$ that all are in the stable core. Since $j_k(i)$ was chosen at random, this situation occurs with probability s^K.
(1) σ_i is updated with a function f_i which depends on variables that all but one are in the stable core. f_i happens to be a Boolean function which is *independent* of the variable outside the stable core, when the $K-1$ variables *in* the core that f_i depends on have their 'stable' values, i.e. the constant values they evolve to. This situation occurs with probability

$$Ks^{K-1}(1-s)p_1,$$

where p_1 is the probability that a random Boolean function of K variables for given values of $K-1$ of the variables is independent of the K'th variable.

.
.
.

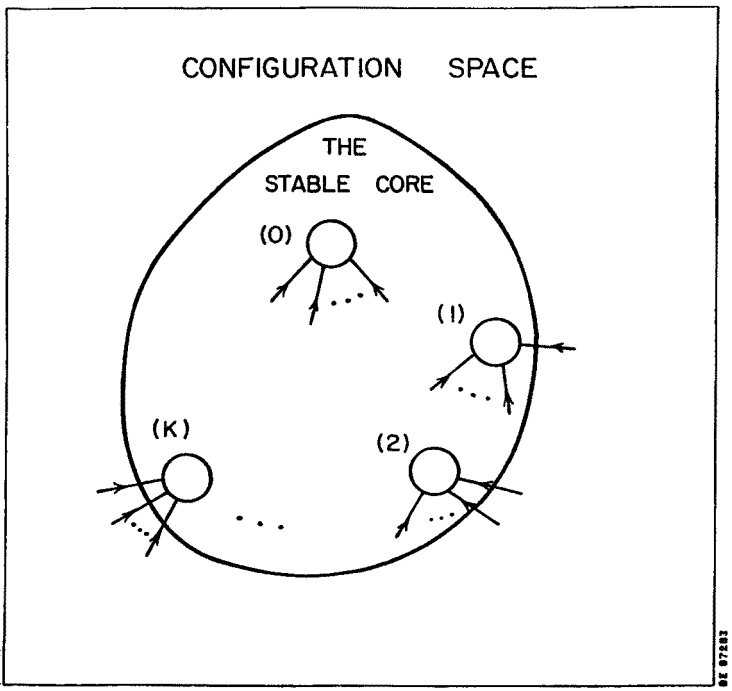

Fig. 8. Symbolic illustration of Eq. (4)

(k) σ_i is updated with a function f_i which depends on variables that all but k are in the stable core. f_i happens to be a Boolean function which is *independent* of the k variables outside the stable core, when the $K-k$ variables *in* the core that f_i depends on have their 'stable' values. This situation occurs with probability

$$\binom{K}{k} s^{K-k}(1-s)^k p_k,$$

where p_k is the probability that a random Boolean function of K variables for given values of $K-k$ of the variables is independent of the other k variables.

.
.
.

(K) ...

Since the relative size s of the stable core is also the probability that a variable σ_i belongs to it, we can sum the probabilities above to an equation for s:

$$s = \sum_{k=0}^{K} \binom{K}{k} s^{K-k}(1-s)^k p_k, \tag{4}$$

where $p_0 = 1$. Clearly $s = 1$ solves Eq. (44) for any values of $p_1, \ldots, p_K$. Division of Eq. (4) by $1-s$ gives

$$s+s^2+ \ldots +s^{K-1} = \sum_{k=1}^{K} \binom{K}{k} s^{K-k}(1-s)^{k-1} p_k. \tag{5}$$

Eq. (5) is also solved by $s = 1$ provided

$$p_1 = 1 - \frac{1}{K}. \tag{6}$$

We shall soon see that this is a critical condition for the network. The slope of the r.h.s. of Eq. (4) at $s = 1$ is $K(1-p_1)$, and at $s = 0$ the r.h.s. equals p_K. Hence, if $p_1 < 1 - 1/K$ there is a second solution to Eq. (4) in the interval $[p_K, 1]$ besides the solution $s = 1$, see Fig. 9.

When there is more than one solution to Eq. (4) in the interval [0, 1], we must look to the time evolution of the network to pick out the relevant solution. We introduce 'the stable core at time t', meaning those variables σ_i which at time t have attained 'stable' values. Let $s(t)$ denote the relative size of the stable core at time t. Then it is clear that $s(t)$ is non-decreasing. It is also clear that $s(1) = p_K$; any variable σ_i updated with a constant function f_i has reached its stable value after one update, no matter what the initial configuration was, and this is the case for only such variables. Finally one may convince oneself that the evolution equation for the stable core is

$$s(t+1) = \sum_{k=0}^{K} \binom{K}{k} s(t)^{K-k}(1-s(t))^k p_k. \tag{7}$$

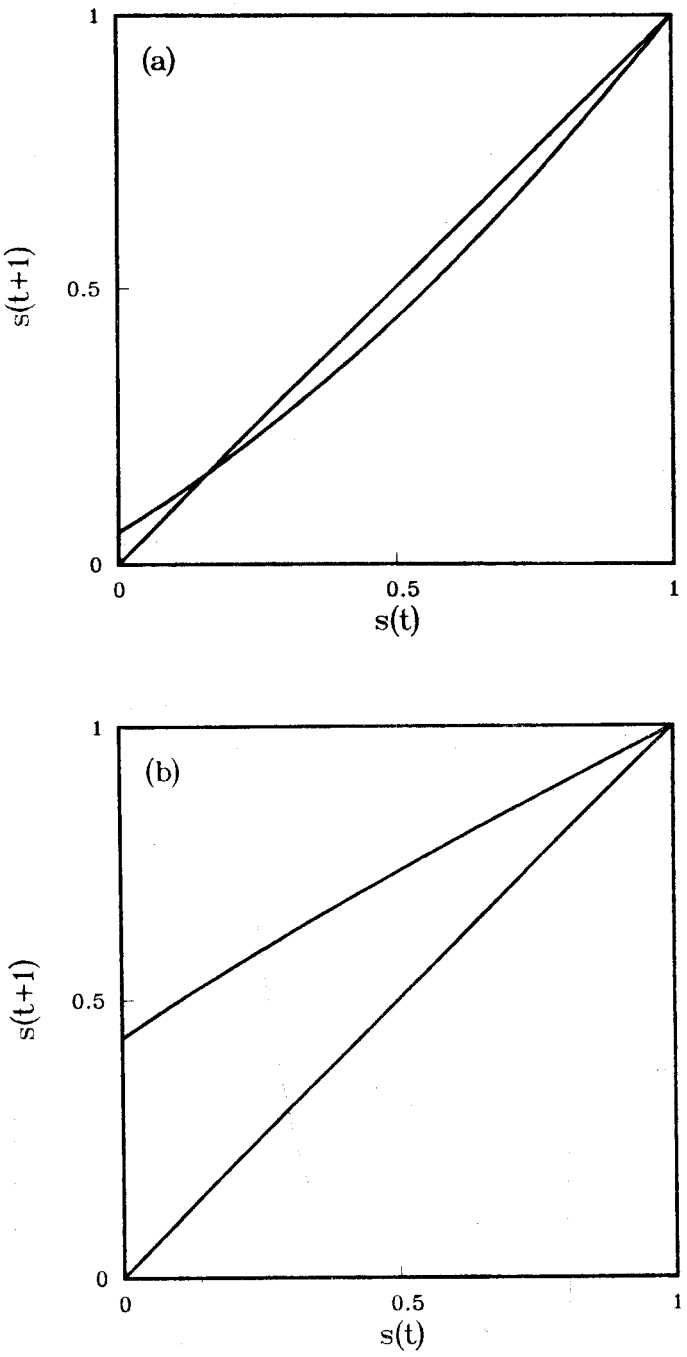

Fig. 9. Graphical representation of Eqs (4) or (7) for $p_1 < 1-1/K$ (a), and $p_1 > 1-1/K$ (b). The curves are for the case $K = 3$, $p = 0.7$ (a), and $p = 0.9$ (b) [23]

The evolution described by this equation is an iterated map. Fig. 9 shows that the smallest of the solutions to the fixed point equation (4) is attractive, hence the relevant one. The two solutions shown change rôle at the value for p_1 given in Eq. (6), which is therefore the critical condition.

When the functions f_i are chosen at random to be 1 with probability p and 0 with probability $1-p$, we find $p_k = p^{2^k}+(1-p)^{2^k}$, and the critical value for p is

$$p_{\text{critical}} = \tfrac{1}{2}\left(1 \pm \sqrt{1-\frac{2}{K}}\right) \quad \text{for} \quad K \geqslant 2. \tag{8}$$

The symmetry w.r.t. $p = 1/2$ in Eq. (8) is due to the equivalence between the values 0 and 1 for σ. For $K = 1$ critical behavior occurs only for $p_1 = 0$ [19].

A subtlety: p_k was defined essentially as the probability that a random Boolean function of k variables is a constant function. This it is with the probability p_k just given, only if the k variables are *independent*. Suppose in the case (k) described above, some of the k variables *not* in the stable core, happen to be identical. Then p_k is not as given above. In the case $k = 2$ e.g. the function XOR is constant, if its two arguments happen to be the same variable. Fortunately, in the limit $N \to \infty$ we may neglect this complication in the evaluation of p_k, since the probability that *some* of k randomly chosen input variables happen to be identical is $O(k(k-1)/(2N))$.

Fig. 10 shows the size s of the stable core as a function of p in the case $K = 3$. We see two phases: the *frozen* phase characterized by $s = 1$ for $p > p_{\text{critical}} = 0.78867\ldots$, and the *chaotic* phase characterized by $s < 1$ for $p < p_{\text{critical}}$.

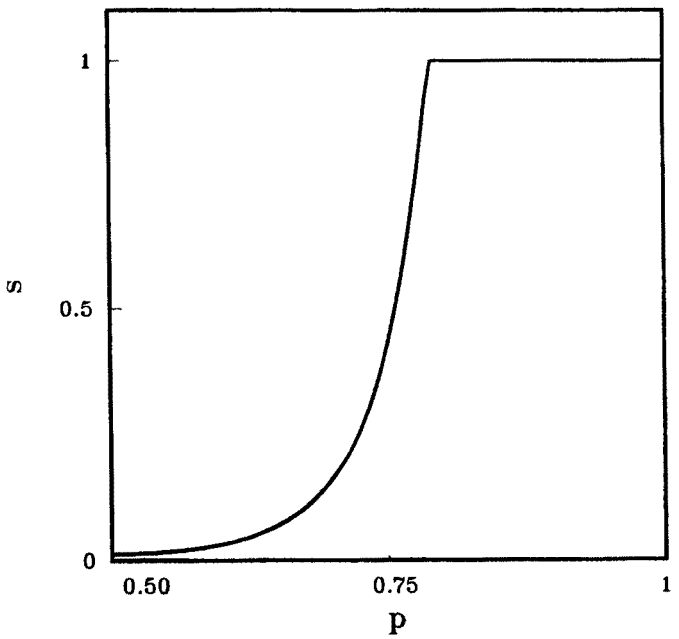

Fig. 10. The size of the stable core as a function of p in the case $K = 3$ [23]

Notice that the time evolution in Eq. (7) is a result of the 'synchronous' or 'parallel' updating of the variables chosen with Eq. (1). But the self-consistency Eq. (4) is independent of the particular time evolution chosen with Eq. (1). Had we instead chosen 'sequential updating', or 'random sequential updating', or any other algorithm that sooner or later will update any variable in the network, then Eq. (4) would still be valid, and consequently so would the phase structure just found.

The recursive reasoning applied here to the size of the stable core applies also to the distribution $P(m)$ of local magnetizations in the network. Define the local magnetization $m_i(t)$ as the sample averaged value of spin i at time t: $m_i(t) = \langle S_i(t) \rangle$. Then we can define $P_t(m)$ as the relative frequency of local magnetizations with value m. P_{t+1} is related to P_t much like $s(t+1)$ is related to $s(t)$. As a matter of fact Eq. (7) is contained in the this relationship [24].

6. *Monte Carlo results for Kauffman's model [10]*

Let us return to Figs 6 and 7. The square in Fig. 6 represents the space of 2^N configurations of a sample network. It is broken into basins of attraction with relative sizes W_s: if Ω_s of the 2^N configurations eventually end up on the s'th limit cycle, then we define

$$W_s = \Omega_s / 2^N. \tag{9}$$

W_s is also called the *weight* of the s'th attractor. Clearly, for each sample network we have

$$1 = \sum_s W_s \tag{10}$$

and the probability that P randomly chosen configurations eventually end up on the same limit cycle is

$$Y_P = \sum_s W_s^P. \tag{11}$$

For the sake of brevity, we write Y_2 as Y. Does the value of Y_p vary from sample to sample? Obviously so, it may seem, since each sample is created with different random connections $(j_1(i), \ldots, j_K(i))_{i=1,\ldots,N}$ and different randomly chosen functions $(f_i)_{i=1,\ldots,N}$. But it is not obvious in the limit $N \to \infty$: Y_P could be a *self averaging* quantity, like the magnetization of a ferromagnet, the pressure of a gas, etc. Alternatively, Y_P could simply be *zero*: suppose the typical number of configurations in a basin of attraction remains finite or grows with N slower than 2^N. Then by Eq. (9) W_s would vanish for infinite N, and Eq. (10) would be satisfied by an infinite sum over infinitesimal weights W_s. For $P > 1$ we would have $\overline{Y_P} = 0$.

Let Π_P denote the frequency distribution for Y_P. Π_P has been studied numerically through its first moments [10]. The first moment of Π_2, written Π, is just $\overline{Y}$. Fig. 11 shows $\overline{Y}$ for $K = 1, 2, 3, 4$ and N ranging from 5 to 240. Except in the case $K = 2$, which from Sect. 5 we know is critical, a limit value seems to be reached by $\overline{Y}$ for large N. Are the finite values for $\overline{Y}$ at $N \approx \infty$ self averaging? The measured standard deviations for Y are shown in Fig. 12. Within the error bar the standard deviations are constant at large N. So we

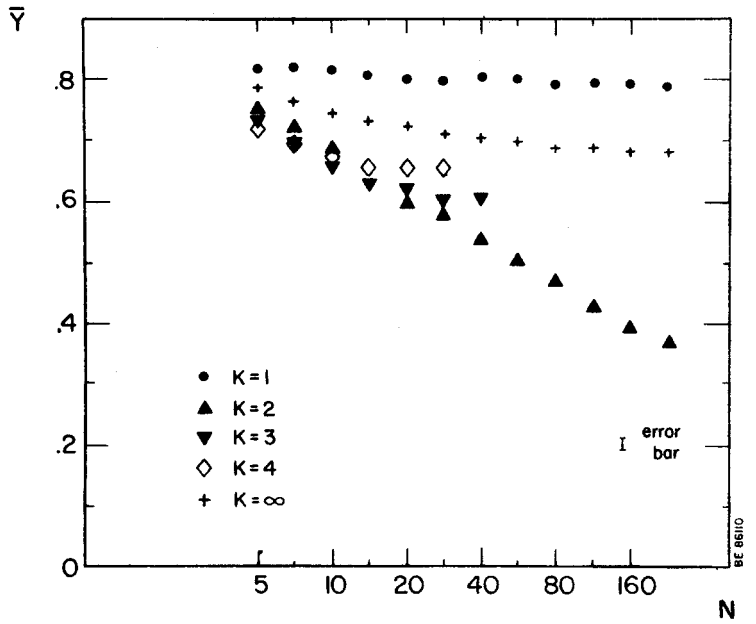

Fig. 11. $\bar{Y}$ versus N for connectivities $K = 1, 2, 3, 4, \infty$. Each point represents an average over 10,000 samples [10], except the crosses, which are exact analytical results for $K = \infty$ [20]

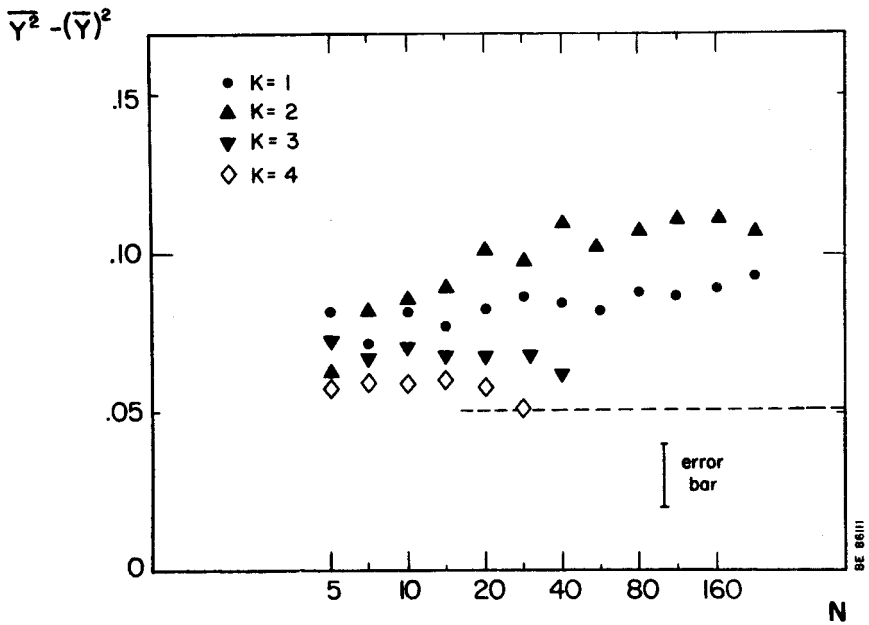

Fig. 12. $\sigma^2(\bar{Y})$ versus N for $K = 1, 2, 3, 4$. Each point represents an average over 10,000 samples [10]. The dashed line represents the value $\lim_{N\to\infty} \lim_{K\to\infty} \sigma^2(\bar{Y}) = \frac{16}{315}$ [20]

conclude that $\overline{Y}$ is not self averaging, except in the case $K = 2$, which is undetermined: if for $K = 2$ $\overline{Y} \to 0$ for $N \to \infty$, the standard deviation for $K = 2$ must also go to zero. In Fig. 12 it does not do this. Neither does it go to a constant value. So N is not large enough, as is often a problem in simulations of critical systems.

After the Monte Carlo simulations discussed here were done, the quantities shown were calculated analytically in the limit K infinite [20]. The results in this limit are also shown in Figs 11 and 12, and show that $\overline{Y}$ is finite and not self averaging. Details about this calculation are given in Sect. 7. Subsequently, $\overline{Y_P}$ and other quantities have been calculated analytically for $K = 1$ [19]. At a critical point $\overline{Y_P}$ and $\overline{Y^n}$ were found to vanish in the limit $N \to \infty$. Some details are given in Sect. 8.

Now look at Fig. 7 and also Figs 13 and 14, which are of a similar kind, and compare the Monte Carlo data for Kauffman's model, shown as points, with the theoretical predictions for the SK-model, shown as full lines. Do the points fall on the lines? Have we found a new universal property, common to very different systems with quenched disorder? Alas, no: the points represent averages over 10,000 statistically independent samples of quantities distributed in the interval [0, 1]. So the standard deviations on the values plotted are smaller than 0.005, which is approximately the size of the plotted points. If this argument does not convince you, look at the one cross in each of the figures 7, 13, and 14. These crosses represent the exact analytical results for the limit K infinite, N infinite, and are *not* on the curves for the SK-model. After the Figures 7, 13, and 14 were made, the quantities shown have also been calculated analytically for the case $K = 1$ [19], and do not coincide with the results for the SK-model either, as we shall see in Sect. 8.

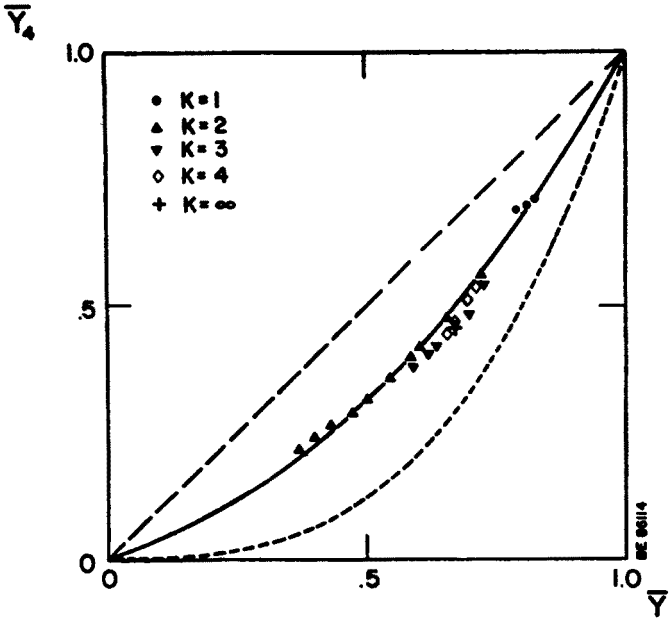

Fig. 13. $\overline{Y_4}$ versus $\overline{Y}$ [10]. Full curve repreesnts $\overline{Y_4} = \overline{Y}(1+\overline{Y})(2+\overline{Y})/6$ [11–14]. Dashed curves are bounds $\overline{Y^3} < \overline{Y_4} < \overline{Y}$. Otherwise like Fig. 7

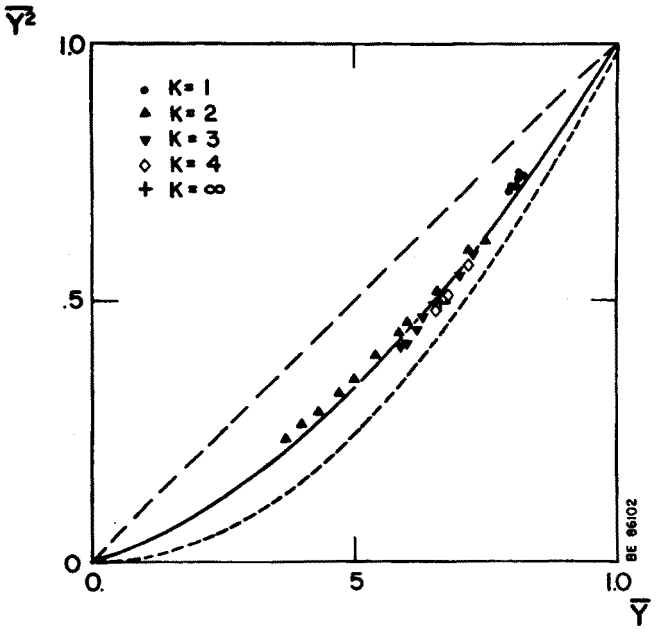

Fig. 14. $\overline{Y^2}$ versus $\overline{Y}$ [10]. Full curve represents $\overline{Y^2} = \overline{Y}(1+2\overline{Y})/3$ [11–14]. Dashed curves are bounds $\overline{Y^2} \leqslant \overline{Y^2} \leqslant \overline{Y}$. Otherwise like Fig. 7

All is not lost, however; it may still be possible to find universal properties in these models: the Monte Carlo results just discussed were all measured with the probability p set to the value 1/2. For that value of p Kauffman's model is in its frozen phase for $K = 1$, critical for $K = 2$, and in its chaotic phase for $K = 3, 4, \ldots$ One may have more success finding universal behavior, if networks with different connectivities K are compared at equivalent rather than identical values of p, e.g. at the critical values given in Eq. (8). This has not been done. What would one find? The results for $K = 2$, as shown in Figs 7, 11–14 and, hopefully, results for $K = 3, 4, \ldots$ on top of a line connecting the results for $K = 2$. The latter results differ at most a few standard deviations from the curves for the SK-model, though in a systematic way. But even if Kauffman's model at its critical points does differ from the SK-model in its multi-valley structure, it would be a very nice result if this structure showed universal behavior in its dependence on K and finite N.

How is such a Monte Carlo simulation done? As follows: choose values for N and K. Generate random connections $j_k(i)$ in $\{1, \ldots, N\}$ for $k = 1, \ldots, K$ and $i = 1, \ldots, N$, and choose for $i = 1, \ldots, N$ and *input* $= 1, \ldots, 2^K$ $f_i(input)$ at random in $\{0, 1\}$ with probability p for the value one. The variable *input* enumerates the 2^N possible different inputs to $f_i \cdot j_k(i)$ and $f_k(input)$ are stored in arrays, and represent a sample network. Since Y_P is the probability that P randomly chosen configurations eventually end up on the same limit cycle, that is exactly how it can be measured for P not too large: choose P configurations at random, and compute their time evolution using Eq. (1). Do so for many sample networks. The frequency with which all P points end up on the same limit cycle is an estimate for $\overline{Y_P}$.

In the chaotic phase typical transients and limit cycles have lengths that grow exponentially with N. This is connected with the fact that $\overline{Y_P}$ remains finite for increasing N. This sets low limits on the values of N that can be handled in a simulation in the chaotic phase, see e.g. Fig. 11. At the critical point, on the other hand, $\overline{Y_P}$ drops with increasing N (at least for $K = 1$ (Sect. 8) and $K = 2$), hence simulations of larger systems are *easier* at the critical points!

7. $K = \infty$: *the random map model* [20, 21]

When the connectivity K of Kauffman's model is sent to infinity, the dynamical law of any sample is a random map in configuration space. Consequently a number of quantities, including those measured in Monte Carlo simulations and discussed in the previous Section, become calculable analytically [20]. This is very nice, since the Monte Carlo results are not entirely satisfying because of statistical errors and finite size effects. Conclusions about quantities measured at finite N, e.g. absence of self averaging of Y_P, become more convincing, when supported by exact results for infinite N, even if the latter results are available only for $K = \infty$.

Let us see why $K = \infty$ makes the dynamical law (1) a random map: first remember that K is the number of randomly chosen inputs $j_1(i), \ldots, j_K(i)$ to any variable i. Any value j may occur more than once among the K inputs to variable i, and for N finite, K infinite, every possible value of j in $\{1, \ldots, N\}$ occurs, i.e. f_i depends on *every* variable $\sigma_j, j = 1, \ldots, N$, or, equivalently, on the entire configuration in question: $f_i = f_i(\sigma)$. Every configuration $(\sigma_i)_{i=1,\ldots,N}$ may be identified with an integer $\#[\sigma]$ between zero and $2^N - 1$, e.g. by letting the value of the i'th variable σ_i be the i'th binary digit of the number:

$$\#[\sigma] = \sum_{i=1}^{N} \sigma_i 2^{N-i}. \tag{12}$$

So when $f_i(\sigma)$ is assigned a random value, 0 or 1 equiprobably, this value is the i'th binary digit of the configuration σ' that σ is mapped into. Since each digit of σ' is chosen at random in $\{0, 1\}$, so is σ' in $\{0, 1, \ldots, 2^{N-1}\}$, and we conclude f is the random map.

Now let us compute $\overline{Y_P}$: we define $Q(T_1, T_2, \ldots, T_P)$ as the probability that a randomly chosen configuration C_1 visits T_1 different points in configuration space before revisiting any of these T_1 points, that a randomly chosen configuration C_2 visits T_2 different points in configuration space before falling on the trajectory of C_1, that a randomly chosen configuration C_3 visits T_3 different points in configuration space before falling on the union of trajectories of C_1 and C_2, ..., that a randomly chosen configuration C_P visits T_P different points in configuration space before falling on the union of trajectories of $C_1, C_2, \ldots, C_{P-1}$. With a configuration space of M points it is not difficult to see that [20]

$$Q(T_1, T_2, \ldots, T_P) = \left(1 - \frac{1}{M}\right)\left(1 - \frac{2}{M}\right) \cdots \left(1 - \frac{T_1 + T_2 + \ldots + T_{P-1}}{M}\right)$$
$$\times \frac{T_1^2}{M^2} \frac{T_1 + T_2}{M} \cdots \frac{T_1 + T_2 + \ldots + T_{P-1}}{M} \tag{13}$$

and

$$\overline{Y_P} = \sum_{T_1=1}^{M} \sum_{T_2=0}^{M-T_1} \cdots \sum_{T_P=0}^{M-T_1 \cdots -T_{P-1}} Q(T_1, T_2, \ldots, T_P). \tag{14}$$

Changing variables to

$$S_i = \sum_{j=1}^{i} T_j \tag{15}$$

Eqs (13) and (14) give

$$\overline{Y_P} = \sum_{S_P=1}^{M} \sum_{S_{P-1}=1}^{S_P} \cdots \sum_{S_1=1}^{S_2} \frac{S_1^2}{M^2} \frac{S_2}{M} \frac{S_3}{M} \cdots \frac{S_{P-1}}{M} \left(1-\frac{1}{M}\right)\left(1-\frac{2}{M}\right) \cdots \left(1-\frac{S_{P-1}}{M}\right). \tag{16}$$

In the limit M infinite one can use continuous variables

$$S_i = \sqrt{M}\, t_i, \quad 1 = \sqrt{M}\, dt_i \tag{17}$$

and Eq. (16) becomes

$$\overline{Y_P} = \int_0^\infty dt_P \exp(-t_P^2/2) \int_0^{t_P} dt_{P-1} t_{P-1} \int_0^{t_{P-1}} dt_{P-2} t_{P-2} \cdots \int_0^{t_2} dt_1 t_1^2 \tag{18}$$

which is easily integrated to

$$\overline{Y_P} = \frac{4^{P-1}((P-1)!)^2}{(2P-1)!} = \frac{\Gamma(P)\Gamma(1/2)}{2\Gamma(P+1/2)} = 1/2\, B(P, 1/2),$$

$$\overline{Y_2} = 2/3, \quad \overline{Y_3} = 8/15, \quad \overline{Y_4} = 16/35, \quad \overline{Y_5} = 128/315, \text{ etc.}, \tag{19}$$

where $B(y, z)$ is Euler's integral of the first kind. For a given sample of the network, i.e. for a given random map, the probability Y_P that P randomly chosen configurations belong to the same basin of attraction is

$$Y_P = \sum_s W_s^P = \int_0^1 dW W^P \sum_s \delta(W - W_s). \tag{20}$$

Hence, when averaging over all samples, we have

$$\overline{Y_P} = \int_0^1 dW W^P f(W), \tag{21}$$

where

$$f(W) = \overline{\sum_s \delta(W - W_s)} \tag{22}$$

i.e. $f(W)$ is the frequency of basins of attraction with relative size W. The probability that a randomly chosen configuration belongs to a basin of size W is

$$g(W) = W f(W). \tag{23}$$

$g(W)$ is of course a normalized probability distribution in $[0, W]$. From Eq. (21) we see that $\overline{Y_{P+1}}$ is the P'th moment of $g(W)$. $\overline{Y_P}$ is given in Eq. (19), and it is possible to find $g(W)$ from its moments: using

$$B(y, z) = \int_0^1 dW W^{y-1}(1-W)^{z-1} \tag{24}$$

in Eq. (19) we get [20]

$$g(W) = \frac{1}{2\sqrt{1-W}}. \tag{25}$$

In the SK-model $g(W)$ is [12]

$$g_{SK}(W) = \frac{W^{y-1}(1-W)^{-y}}{\Gamma(y)\Gamma(1-y)}. \tag{26}$$

The parameter y is just the first moment $\overline{Y}$. When $y = 2/3$, which is the value for $\overline{Y}$ in Kauffman's model with $K = \infty$, $g(W)$ for the two models have almost, but not exactly, the same shape. This explains why the higher moments for the two models almost coincide, but also *proves* that the multi-valley structure of the two models is *not* identical, despite the striking similarity we have seen.

From the knowledge of $g(W)$ one may easily compute $g(W_1, W_2)$, the probability that two randomly chosen configurations fall on attractors with weights W_1 and W_2, and similarly $g(W_1, W_2, W_3)$ and from them $\overline{Y_2}$ and $\overline{Y_3}$ [20]. This can be done also for finite N; the results are shown in Figs 11–14. Notice in particular in Fig. 12 that $\sigma(Y)$ remains finite in the limit $N \to \infty$, and its value is close to those found in simulations for $K = 3$ and $K = 4$. We conclude that Y is *not* self averaging for K infinite, and feel rather convinced that neither is it for $K = 3, 4, \ldots$

Now let us compute $\Pi(Y)$ itself: if we consider a configuration C, we know that the probability that it belongs to a basin of weight W is $g(W)$. Configuration space may be viewed as composed of the basin that C belongs to — it consists of $M \cdot W$ configurations — and of its complement of $M \cdot (1-W)$ configurations. The restriction $\tilde{T}$ of the random map T to this complement is also a random map and therefore has the same statistical properties as the map T. Consequently we have

$$Y = W^2 + (1-W)^2 \tilde{Y}, \tag{27}$$

where Y refers to the map T and $\tilde{Y}$ to the map $\tilde{T}$. Notice W and $\tilde{Y}$ are independent variables, distributed with probabilities $g(W)$ and $\Pi(\tilde{Y})$. Consequently

$$\Pi(Y) = \int_0^1 dW g(W) \int_0^1 d\tilde{Y} \Pi(\tilde{Y}) \delta(Y - W^2 - (1-W)^2 \tilde{Y}). \tag{28}$$

In this equation we know g; Π is the unknown. We have not been able to solve for Π analytically. From Eq. (28), or by taking the average of powers of both sides of Eq. (27), we can find a recursion relation which gives us all moments of Π. But this moment problem we have not been able to solve. We can easily find Π numerically, however, using a stochastic method based on Eq. (27): we generate recursively a random sequence $\{y_n\}$ by choosing

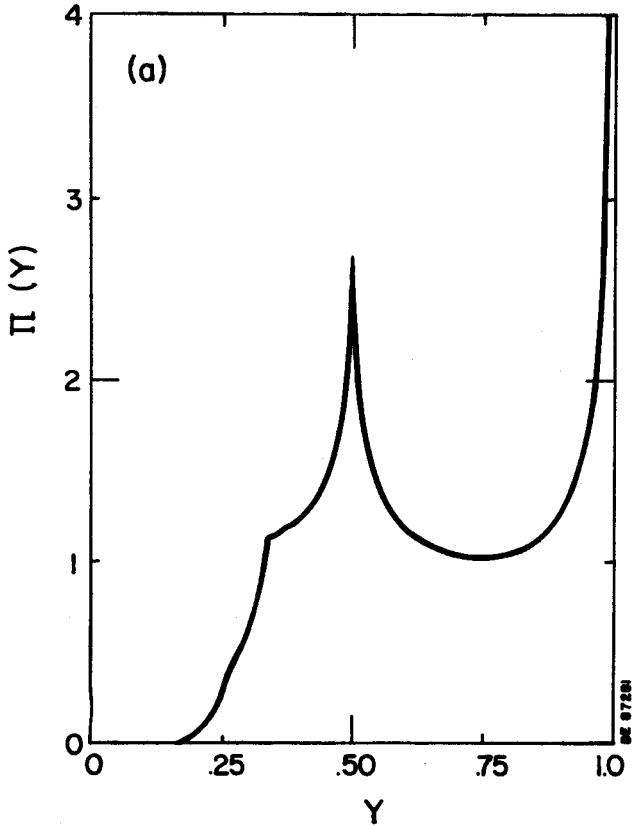

Fig. 15a

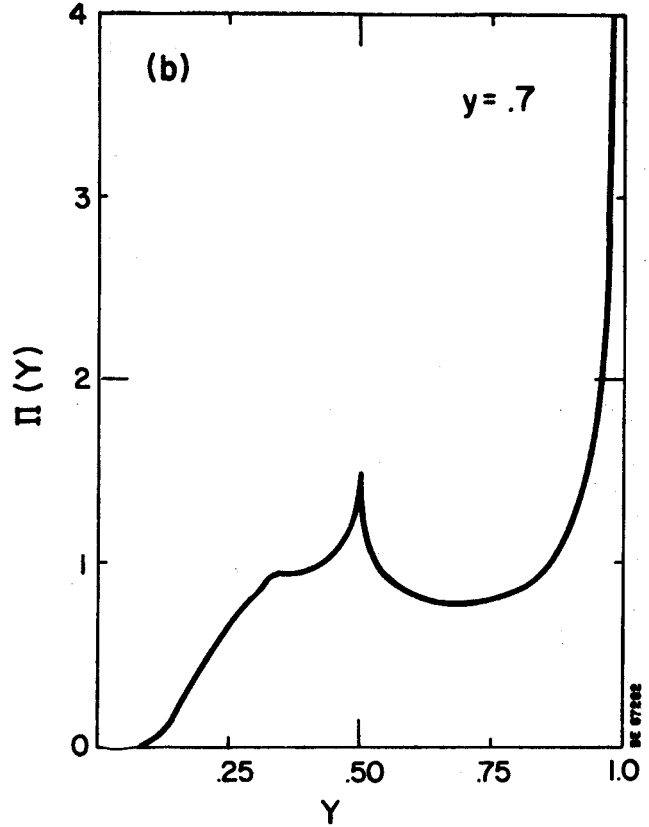

Fig. 15b

Fig. 15. $\Pi(Y)$ for the random map (a), and for the SK-model (b) [21]

y_0 at random in [0, 1], and by computing y_{n+1} from y_n using

$$y_{n+1} = W_n^2 + (1 - W_n)^2 y_n, \tag{29}$$

where W_n is randomly chosen with distribution $g(W_n)$. The values y_n generated this way are distributed according to Π. Fig. 15a is a histogram based on 10,000,000 values. It shows singularities in $\Pi(Y)$ at $Y = 1, 1/2, 1/3$, and $1/4$. It has been shown that $\Pi(Y)$ has singularities at $Y = 1/n$, $n = 1, 2, \ldots$ *and* that this is a quite general feature of randomly broken objects [21].

For the SK-model $\Pi(Y)$ was found to have the shape shown in Fig. 15b for parameter value $y = 0.7$. The similarity between the two functions $\Pi(Y)$ is striking. It is explained by the fact that main features of $\Pi(Y)$ are independent of the particular properties of the two models, but depend only on the property that configuration space in both cases is a randomly broken object with approximately the same bias towards large pieces [21]. This also explains, why the second moments $\overline{Y_3}$ for the two models almost coincide, when the first moments $\overline{Y_2}$ do so.

It is nice to have exact results for $K = \infty$; but it would be even nicer to have an expansion scheme, say in $1/K$, with the results for $K = \infty$ as the first term. The Monte Carlo data for $K = 4$ compared with the exact results for $K = \infty$ indicate that 4 is close to infinity. So an expansion scheme might successfully describe most of the chaotic phase. We do not know how to design such a scheme.

8. $K = 1$: *another solvable case* [19]

In the previous Section we presented exact results for Kauffman's model deep in its chaotic phase. In the present Section we shall present exact results in the frozen phase. This is possible for $K = 1$ and for any value of p. The results are obtained as rapidly converging sums over classes of samples. These sums are somewhat similar to those obtained by high temperature expansion of lattice spin systems and by strong coupling expansion of lattice gauge systems. The convergence properties are better in the present case, though: some quantities are obtained exactly by a *finite* number of terms, and the singularity determining the radius of convergence for the infinite sums occurring, is the critical point itself. Furthermore, though not yet fully demonstrated, it looks as if the results thus obtained for $K = 1$ can be used to explain the behavior of Kauffman's model with any connectivity K, anywhere in the frozen phase, and maybe even a little beyond the phase boundary and into the chaotic phase; i.e. critical indices are maybe computable this way. So the exact results for the case $K = 1$ not only complement the results for $K = \infty$, but also hold more promise for further development. Now let us see why this case is analytically tractable:

For $K = 1$ every variable σ_i receives input from only one variable $\sigma_{j(i)}$:

$$\sigma_i(t+1) = f_i(\sigma_{j(i)}(t)), \tag{30}$$

where $j(i)$ was randomly chosen. Thus, for $K = 1$ the connection graph in Fig. 1 is just the graph of a random map among the N variables with its arrows reversed. Such a graph consists of only loops and trees, the trees being rooted in the loops; see Fig. 16. The informa-

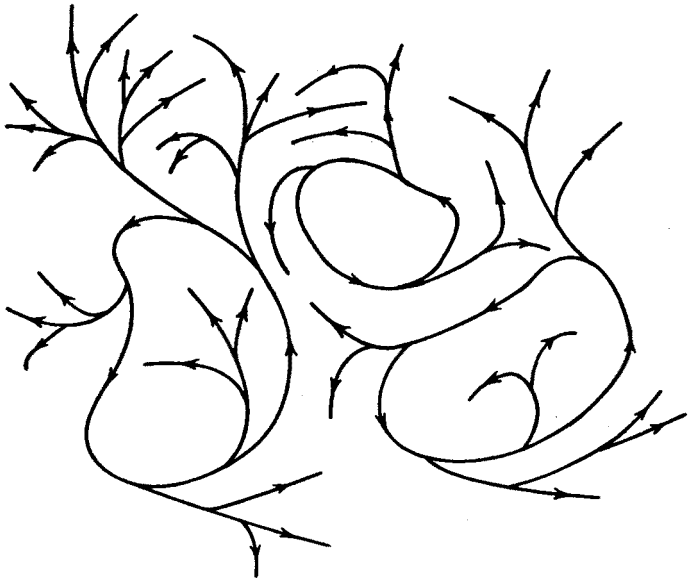

Fig. 16. Connection graph for Kauffman's model with $K = 1$. Each connected part of the graph consists of one loop and trees rooted in this loop

tion contained in initial values $\sigma_i(0)$ placed on trees propagates with time towards the ends of the branches, where it is lost, if it is not lost before by being used as input to a function f_i with constant output. After at most N time steps the only initial values 'remembered' by the network, are those placed on loops, and only those placed on 'information conserving' loops. An information conserving loop is a loop in which only the functions 'identity' and 'negation' occur. The other two Boolean functions of one variable are the constant functions 1 and 0, 'tautology' and 'contradiction'. If any of these two functions occur anywhere in a loop, it is not information conserving, since all initial values for variables on such a loop are 'forgotten', when by Eq. (30) they are used as input to a function with constant output. The functions 'identity' and 'negation', on the other hand, conserve information. One can calculate the probability that a sample of Kauffman's model with $K = 1$ has n_L loops of length L, $L = 1, 2, 3, \ldots$ in its connection graph. With the notation

$$\hat{n} = \sum_{L=1}^{\infty} n_L L \tag{31}$$

it is [19]

$$P(n) = \frac{\hat{n}}{N} \frac{N!}{(N-\hat{n})! N^{\hat{n}}} \prod_{L=1}^{\infty} \frac{L^{-n_L}}{n_L!}$$

$$= \frac{\hat{n}}{N} \exp\left(-\hat{n}^2/(2N)\right) \prod_{L=1}^{\infty} \frac{L^{-n_L}}{n_L!} + O\left(\frac{1}{\sqrt{N}}\right). \tag{32}$$

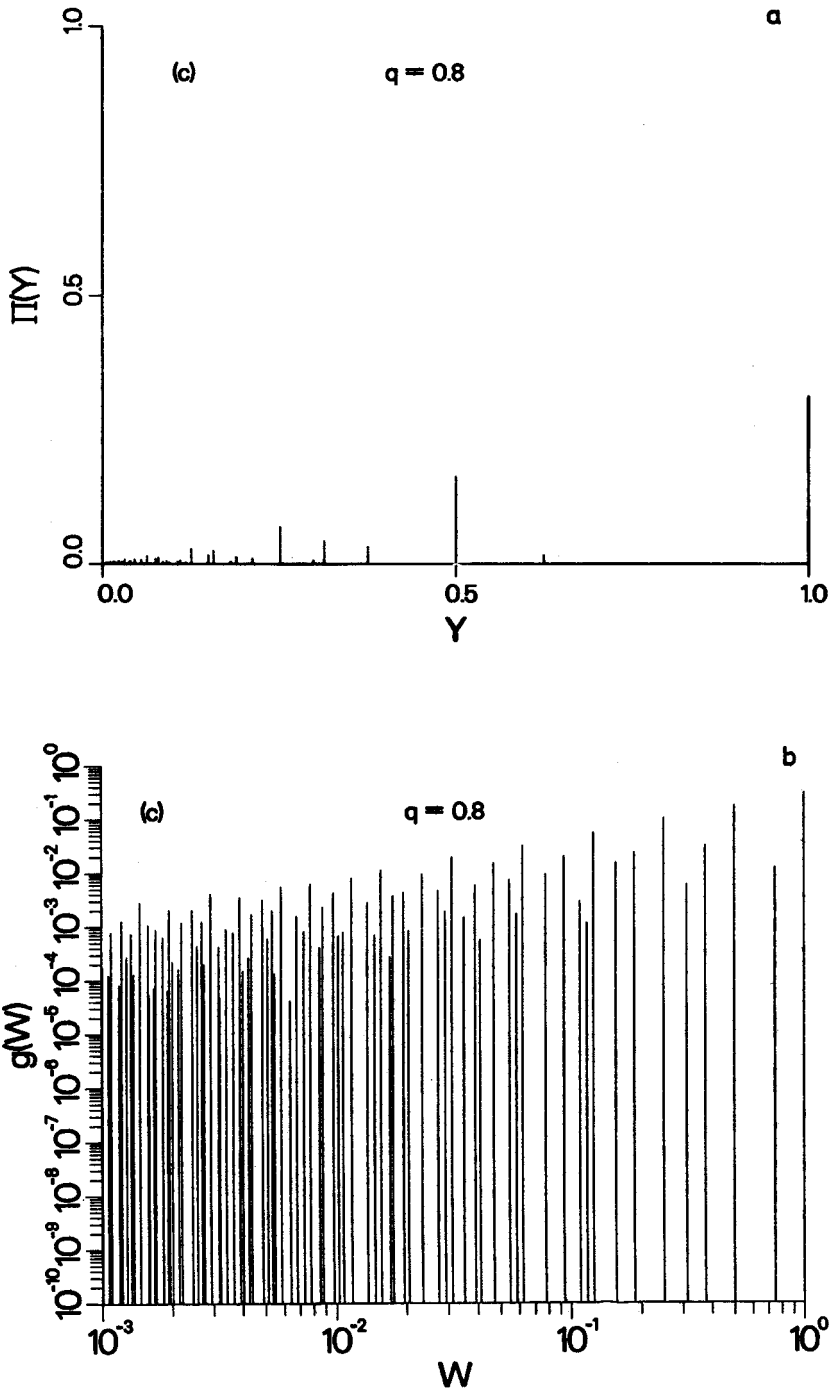

Fig. 17. (a) $g(W)$ for $q = 0.8$. q is a sum of delta functions. Its points of support do not depend on q, and accumulate at $W = 0$ [19]. (b) Same as (a), but with logarithmic axes

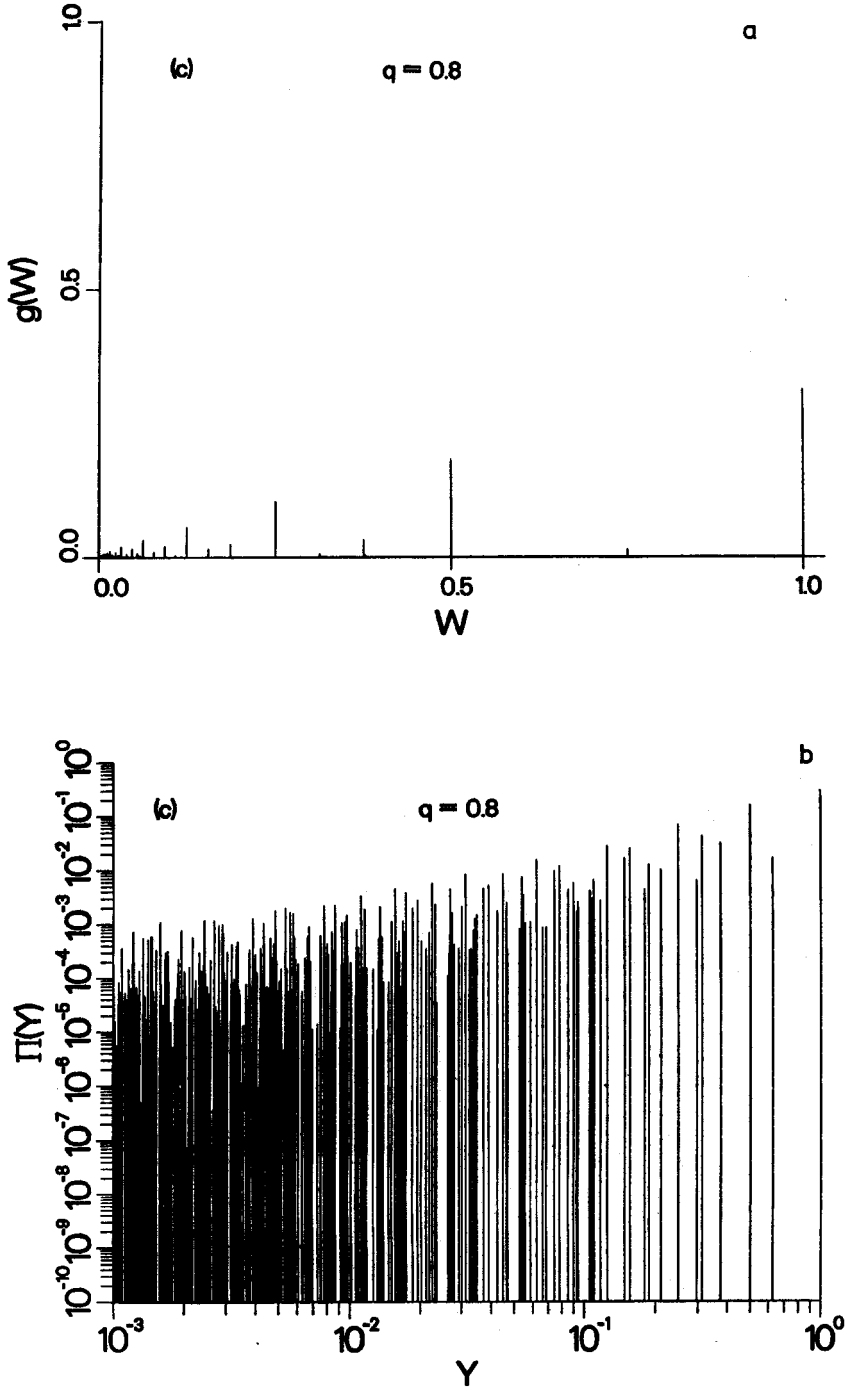

Fig. 18. (a) $\Pi(Y)$ for $q = 0.8$. Π is a sum of delta functions. Its points of support do not depend on q, and accumulate at $Y = 0$ [19]. (b) Same as (a), but with logarithmic axes

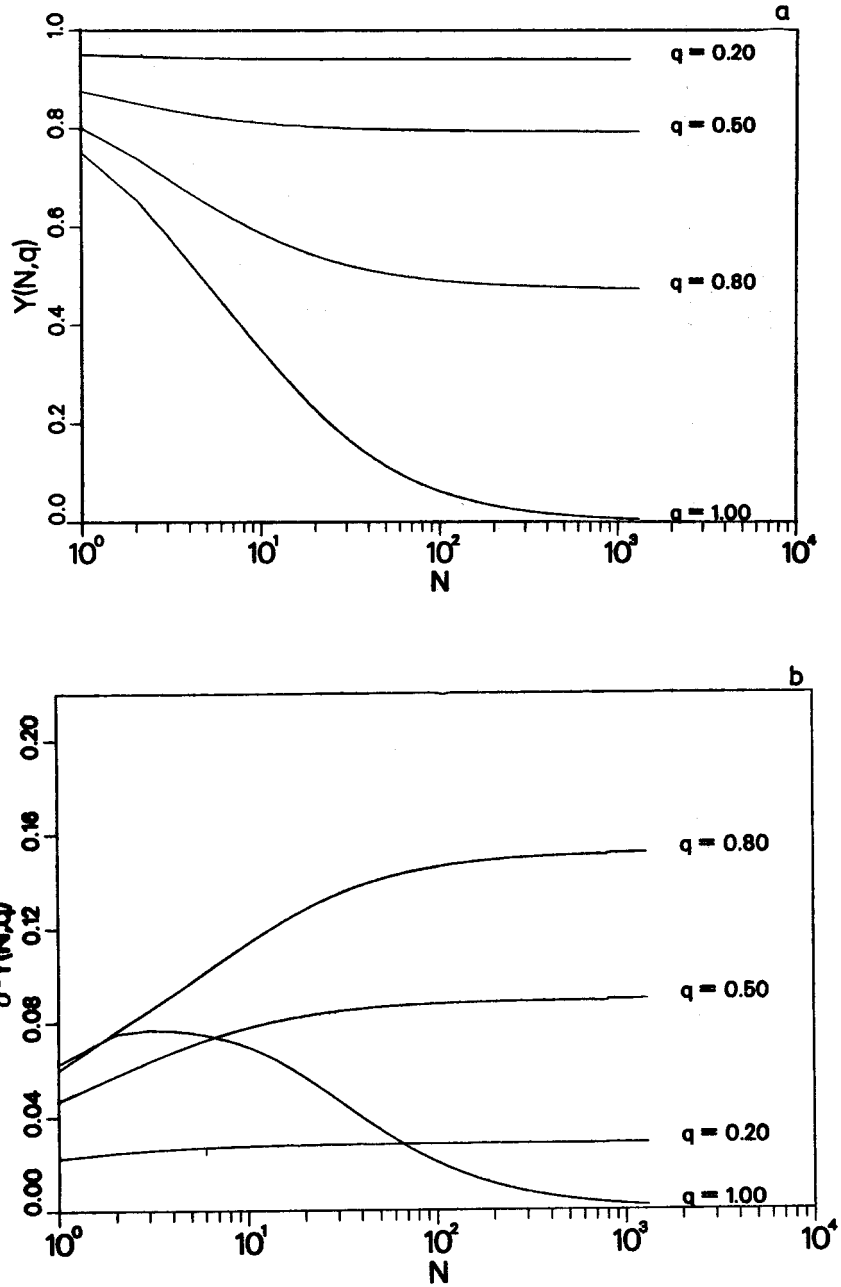

Fig. 19. (a) $\overline{Y}$ as a function of finite network size N for $q = 0.2$, 0.5, 0.8, and the critical case $q = 1$ [19]. (b) $\sigma^2(Y)$ as a function of N for $q = 0.2$, 0.5, 0.8, and 1 [19]

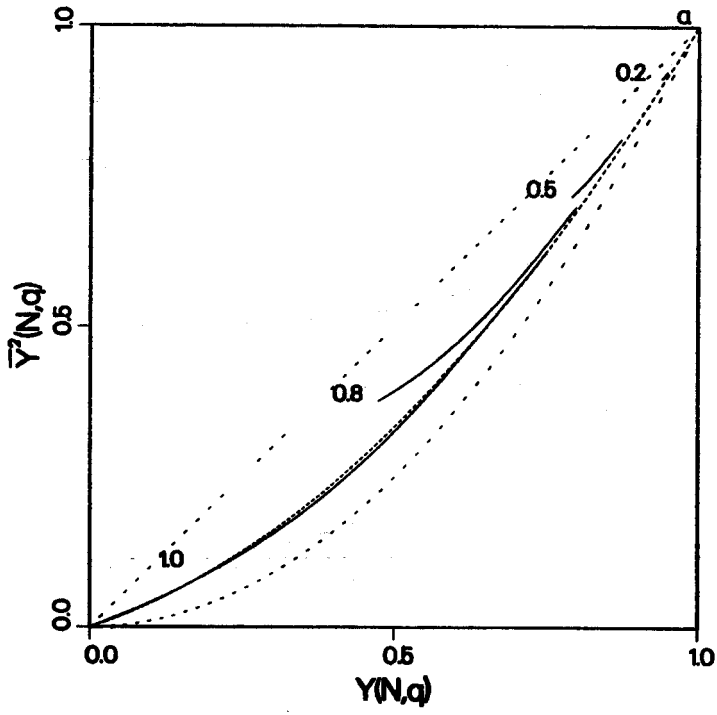
a
1.0
0.5
0.0
0.0
0.5
1.0
$\bar{Y}^2(N,q)$
Y(N,q)
0.2
0.5
0.8
1.0

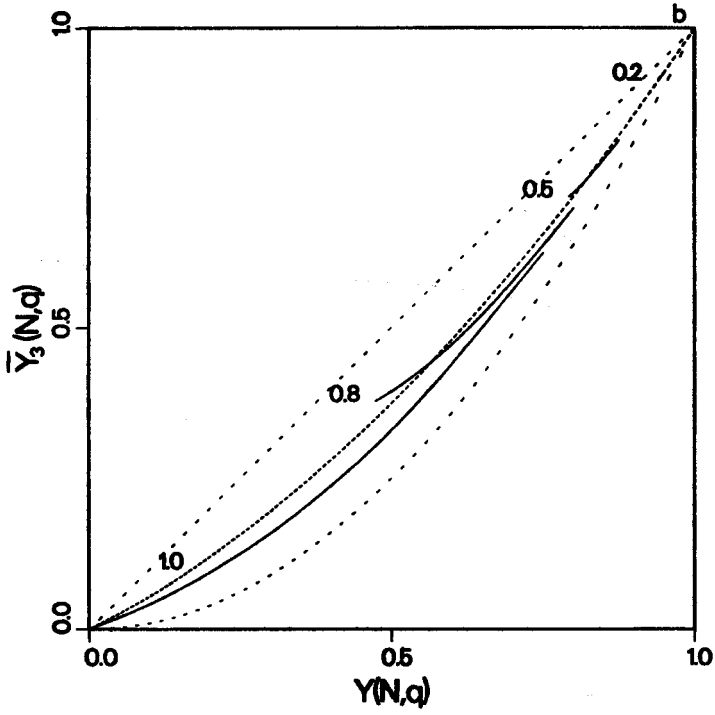
b
1.0
0.5
0.0
0.0
0.5
1.0
$\bar{Y}_3(N,q)$
Y(N,q)
0.2
0.5
0.8
1.0

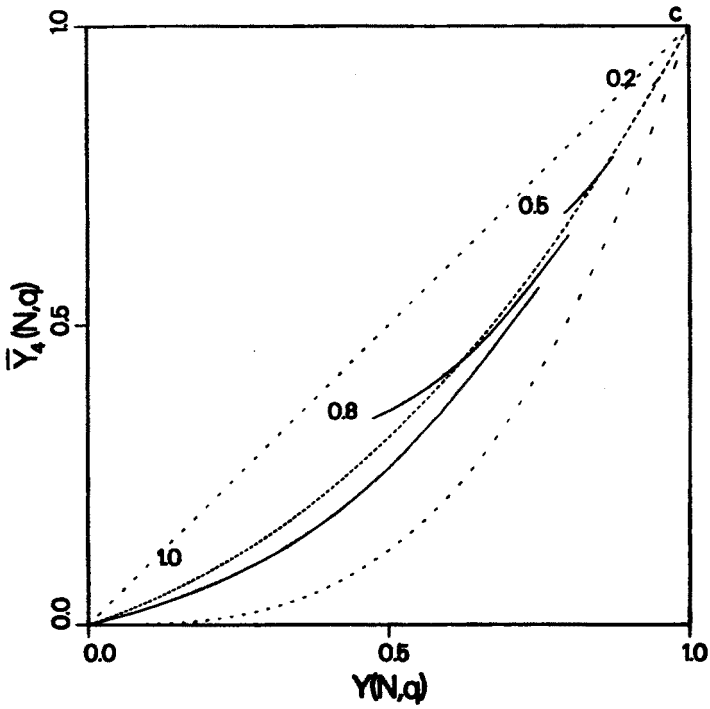

Fig. 20. (a) Full lines: $\overline{Y^2}$ versus $\overline{Y}$ for N varying from 1 to ∞ (making $\overline{Y}$ decrease) and $q = 0.2, 0.5, 0.8$, and 1. Outer dashed lines represent bounds $\overline{Y}^2 < \overline{Y^2} < \overline{Y}$ that are always satisfied. The central dashed line represents the equation $\overline{Y^2} = (\overline{Y}+2\overline{Y}^2)/3$ satisfied by the Sherrington-Kirkpatrick model. (b) $\overline{Y_3}$ versus $\overline{Y}$. Outer dashed lines are bounds $\overline{Y}^2 < \overline{Y_3} < \overline{Y}$, central dashed line the equation $\overline{Y_3} = \overline{Y}(1+\overline{Y})/2$ satisfied by the S-K model. (c) $\overline{Y_4}$ versus $\overline{Y}$. The bounds are $\overline{Y}^3 < \overline{Y_4} < \overline{Y}$, and the result for the S-K model is $\overline{Y_4} = \overline{Y}(1+\overline{Y})(2+\overline{Y})/6$. All three figures are from [19]

We introduce the probability q that the randomly chosen function f_i in Eq. (30) is information conserving. Then the probability that a sample network has m_L information conserving loops of length $L, L = 1, 2, 3, \ldots$ is

$$Q(m) = \sum_{n_1 \geqslant m_1}^{\infty} \sum_{n_2 \geqslant m_2}^{\infty} \ldots P(n) \prod_{L=1}^{\infty} \binom{n_L}{m_L} q^{Lm_L}(1-q^L)^{n_L - m_L}$$

$$= \frac{N!}{(N-\hat{m})!N^{\hat{m}}} q^{\hat{m}} \left(1-q\left(1-\frac{\hat{m}}{N}\right)\right) \prod_{L=1}^{\infty} \frac{L^{-m_L}}{m_L!}, \tag{33}$$

where

$$\hat{m} = \sum_{L=1}^{\infty} m_L L. \tag{34}$$

For N large and $1-q \gg 1/\sqrt{N}$ Eq. (33) becomes

$$Q(m) = (1-q) \prod_{L=1}^{\infty} \frac{1}{m_L!} \left(\frac{q^L}{L} \right)^{m_L} \tag{35}$$

which is a product of independent probability distributions, one for each value of L.

Now we know the probability $Q(m)$ that a sample network has m_L information conserving loops of length L, $L = 1, 2, 3, \ldots$, we may derive the possible values W_s and Y_p can have for such a sample, and the probability with which it has these values. First we observe that the $\hat{m}$ variables on information conserving loops can be in $2^{\hat{m}}$ different configurations. Each of these configurations can be realized by $2^{N-\hat{m}}$ different configurations of the full network. These $2^{N-\hat{m}}$ configurations all belong to the same basin of attraction, since they differ only w.r.t. variables σ_i *not* on information conserving loops, differences which are 'forgotten' after some time. Let us call the variables on information conserving loops *relevant* variables, and the other variables *irrelevant*. Then any configuration, the relevant variables of which go through a cycle of period c, belongs to a basin of attraction containing $c \cdot 2^{N-\hat{m}}$ different configurations, i.e. a basin having weight

$$W = c/2^{\hat{m}}. \tag{36}$$

What remains now is to calculate which cycle lengths c occur for a given set of functions f_i on the information conserving loops. This is tedious combinatorics, which is best left to a computer to carry out, after some simplifications of the task have been made analytically.

A useful theorem states that the maximum value for W that can result from Eq. (36) for given value of $\hat{m}$, decreases faster than $2^{-\hat{m}/2}$ for $m > 7$ [19]. As a consequence $g(W)$ and $\Pi(Y)$ are fully determined in intervals $[W_0, 1]$ and $[Y_0, 1]$ with $W_0 > 0$ and $Y_0 > 0$ by networks characterized by $\hat{m} < \hat{m}_0$, where $\hat{m}_0$ depends on W_0 and Y_0. As a corollary $\overline{Y_p}$ and $\overline{Y^n}$ are computable within exact bounds, which rapidly decrease with increasing $\hat{m}_0$. With $\hat{m}_0 = 23$, the error committed in Figs 17–20 by neglecting networks with $\hat{m} > \hat{m}_0$, is vanishing.

Figure 17 shows $g(W)$ for $q = 0.8$. It is a sum of delta functions with support at $W = 1$, 3/4, 1/2, 3/8, 5/16, 1/4, 3/16, ..., a set of rational numbers with accumulation point $W = 0$. The probabilities g_i for these weights W_i vanish for q approaching one, in such a way that $g(W)$ approaches $\delta(W)$. Figure 18 shows similar properties for $\Pi(Y)$. $q = 1$ is a critical value at which infinitely long loops become information conserving, thus breaking configuration space into infinitesimal basins of attraction. This is clearly seen in Fig. 19, which should be compared with Figs 11 and 12. Fig. 19b shows that $Y(q)$ is not self averaging for $q < 1$, for $N \to \infty$, since $\sigma^2(Y)$ does not vanish in this limit. Fig. 19 also shows that $Y(q = 1)$ vanishes for $N \to \infty$. Finally, Fig. 20abc shows $\overline{Y^2}$, $\overline{Y_3}$, and $\overline{Y_4}$ as functions of $\overline{Y}$ for various values of N and q. These figures should be compared with Figs 14, 7, and 13. We see that it is a coincidence that the results for $q = 1/2$ (i.e. $p = 1/2$) fall on top of the curves for the SK-model. Results for other q-values do not do this.

9. Conclusion

We have seen that random networks of automata are disordered systems with quenched, random dynamics. On the one hand, they are sufficiently simple to make a number of analytical results possible, and simulations fairly easy to do. On the other hand, we have seen that they have properties in common with the complex thermodynamical system that a spin glass is. This similarity between such disparate systems shows that some manifestations of disorder are rather universal.

It is too early to make conclusions about random networks. New analytical results appear to be within reach. Using the size of the stable core as order parameter seems a promising approach. Critical exponents and many network properties in the frozen phase may be computable as due to fluctuations in the size of the stable core. So, although Kauffman's model is a rather primitive system, every new exact result increases its value as a non-trivial, solvable model.

In different forms these lectures were held at The Niels Bohr Institute and NORDITA and at the XXVIII Cracow School of Theoretical Physics in Zakopane. I thank the organizers of the latter for a very pleasant school.

REFERENCES

[1] S. A. Kauffman, *J. Theor. Biol.* **22**, 437 (1969).
[2] S. A. Kauffman, *Math. Life Sci.* **3**, 63 (1970).
[3] S. Wolfram, *Rev. Mod. Phys.* **55**, 601 (1983).
[4] H. Atlan, F. Fogelman-Soulié, J. Salomon, G. Weisbuch, *Cybernetics and Systems* **12**, 103 (1982); F. Fogelman-Soulié, E. Goles-Chacc, G. Weisbuch, *Bull. Math. Biol.* **44**, 715 (1982).
[5] B. Derrida, D. Stauffer, *Europhys. Lett.* **2**, 739 (1986).
[6] G. Weisbuch, D. Stauffer, *J. Phys. (France)* **48**, 11 (1987).
[7] D. d'Humières, Y. Pomeau, P. Lallemand, *C. P. Acad. Sci. Paris* **301**, 139 (1985).
[8] D. Sherrington, S. Kirkpatrick, *Phys. Rev. Lett.* **32**, 1792 (1975).
[9] J. Hertz, *Phys. Scr.* **T10**, 1 (1985).
[10] B. Derrida, H. Flyvbjerg, *J. Phys. A: Math. Gen.* **19**, L1003 (1986).
[11] M. Mézard, G. Parisi, N. Sourlas, G. Toulouse, M. Virasoro, *Phys. Rev. Lett.* **52**, 1146 (1984).
[12] M. Mézard, G. Parisi, N. Sourlas, G. Toulouse, M. Virasoro, *J. Phys. (France)* **45**, 843 (1984).
[13] M. Mézard, G. Parisi, M. Virasoro, *J. Phys. Lett.* **46**, 217 (1985).
[14] B. Derrida, G. Toulouse, *J. Phys. Lett.* **46**, 223 (1985).
[15] B. Lautrup, *The Theory of the Hopfield Model*, lecture notes, Niels Bohr Institute, 1988.
[16] D. O. Hebb, *The Organization of Behavior*, Wiley, New York 1949.
[17] B. Derrida, Y. Pomeau, *Europhys. Lett.* **1**, 45 (1986).
[18] H. J. Hilhorst, M. Nijmeijer, *J. Phys. (France)* **48**, 185 (1987).
[19] H. Flyvbjerg, N. J. Kjaer, *J. Phys. A: Math* **21**, 1695 (1988).
[20] B. Derrida, H. Flyvbjerg, *J. Phys. (France)* **48**, 971 (1987).
[21] B. Derrida, H. Flyvbjerg, *J. Phys. A: Math. Gen.* **20**, 5273 (1987).
[22] B. Derrida, E. Gardner, A. Zippelius, *Europhys. Lett.* **4**, 167 (1987).
[23] H. Flyvbjerg, *J. Phys. A: Math. Gen.*, to appear.
[24] B. Derrida, H. Flyvbjerg, *J. Phys. A: Math. Gen.* **20**, L1107 (1987).